AI-AEC-12887
GENERAL,
MISCELLANEOUS,
AND PROGRESS
REPORTS

QUARTERLY TECHNICAL PROGRESS REPORT
AEC UNCLASSIFIED PROGRAMS
JULY–SEPTEMBER 1969

The preceding Quarterly Technical Progress Report
Is AI-AEC-12860

Atomics International
North American Rockwell

CONTRACT: AT(04-3)-701
ISSUED:

DISTRIBUTION

This report has been distributed according to the category "General, Miscellaneous, and Progress Reports" as given in the Standard Distribution for Unclassified Scientific and Technical Reports, TID-4500.

CONTENTS

Blank Page

Program:	Fast Reactor Development
AEC Task:	6-G, Nuclear Safety (Kinetics), Boiling Studies for Sodium Reactor Safety
Project Manager:	H. A. Morewitz
Reporting Period:	July-September 1969
General Order: 7702	Subaccount: 13410 AEC Category: 04-60-01-09.1

Principal Investigators: D. Logan, J. Landoni, and C. Baroczy

10/4/71

I. PROJECT OBJECTIVES

The general objective of this project is to develop basic information on two-phase flow and boiling required in the safety evaluation of LMFBR designs. This information is important because of the key role that sodium boiling plays in reactor dynamics, in fuel meltdown accidents, and in the ultimate shutdown mechanism of the reactor. Specific objectives of the experimental program include the development of reliable high-flux heaters; and the measurements of boiling heat transfer characteristics, two-phase pressure drop, void fraction, liquid superheating, transient voiding rates and pressures in single channels, and hydrodynamic instabilities. Specific objectives of the theoretical study, in addition to any analyses required to support the experimental work, are: the development of digital computer codes which will predict transient void fraction, flowrate, and heat transfer for single and multichannel sodium flow; and the incorporation of these codes into a general reactor kinetics code.

II. MAJOR ACCOMPLISHMENTS DURING FISCAL YEAR 1970

A total of 374 sodium liquid superheat test runs were completed for test conditions of 5 psia and for fluid velocities of 3 to 9 ft/sec. Included were 50 flow coastdown runs in which boiling was initiated by a reduction in flowrate at otherwise fixed conditions.

A 30-in. shaped heat flux heater was fabricated and tested to a heat flux of 10^6 Btu/hr-ft^2.

A three channel test section flow distributor insert has been fabricated and instrumented in preparation for the three channel experimental program.

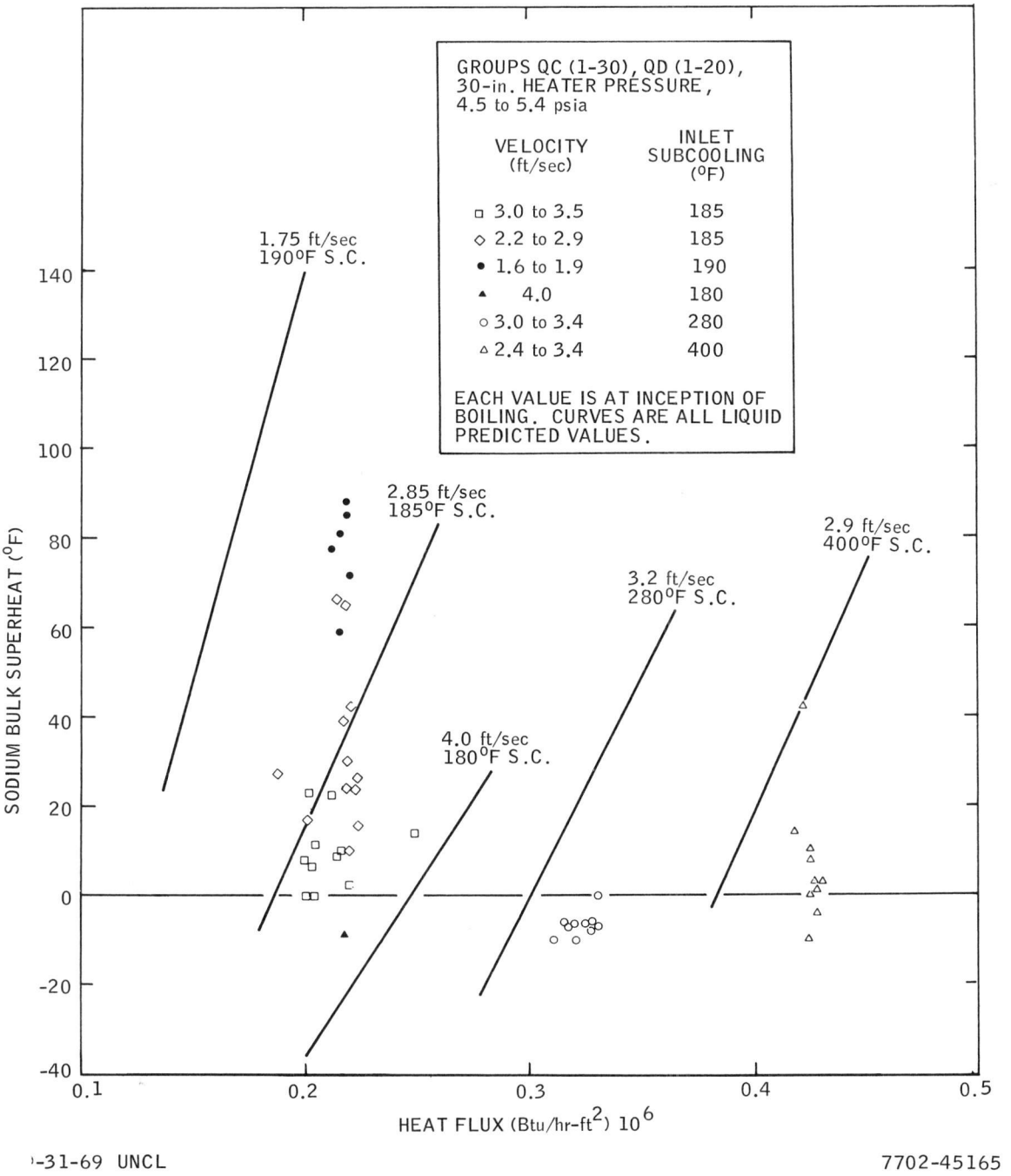

Figure 1. Sodium Superheat Temperature vs Heat Flux

III. PROGRESS DURING REPORT PERIOD

A. SODIUM-LIQUID SUPERHEATING

Sodium-liquid superheat tests are being run to determine the extent of liquid superheating required to initiate boiling in a single LMFBR coolant channel as influenced by parameters such as velocity, heat flux, subcooling, coolant purity, pressure, heater surface finish, etc.

During this report period 374 runs were made. Two hundred and seventy-four of these runs are listed in the table together with 26 runs made last report period. The data on 100 runs have not been reduced yet and will be reported next quarter. Each of these runs were made at a test section pressure of approximately 5 psia. The objective of making runs PD-1 through QB-50 was to study velocity effects. Runs QC-1 through QD-20 (fifty runs) were flow coastdown runs and were made to study transient flow effects on superheating.

Figure 1 is a plot of sodium bulk superheat temperature vs heat flux for the initial flow coastdown experiments consisting of 50 runs, Groups QC (1-30) and QD (1-20). Comparison of the data obtained at boiling inception with all-liquid predictions shows generally good agreement except for the runs taken at the lowest velocity (about 1.75 ft/sec). For these conditions, the predicted bulk superheat is substantially greater than that measured. For the data taken at a heat flux of about 0.2×10^6 Btu/hr-ft^2 at essentially constant inlet subcooling and pressure level, it can be seen that bulk superheat decreases consistently as sodium velocity increases over the range 1.6 to 1.9 ft/sec, to 4 ft/sec. This trend is in agreement with that shown by the all-liquid predictions for these data, and confirms both the previously obtained data and predicted trends as described in AI-AEC-12767. This initial examination of the superheat data, taken under moderate transient flow conditions in which boiling was achieved approximately 26 sec after the start of flow reduction, indicates that these data are very similar to those previously obtained under steady flow conditions.

The effect of velocity on superheat is more clearly seen in Figure 2. The data points shown are those of Figure 1 at a constant heat flux of about 0.21×10^6 Btu/hr-ft^2, and an approximately constant inlet subcooling of about 185°F.

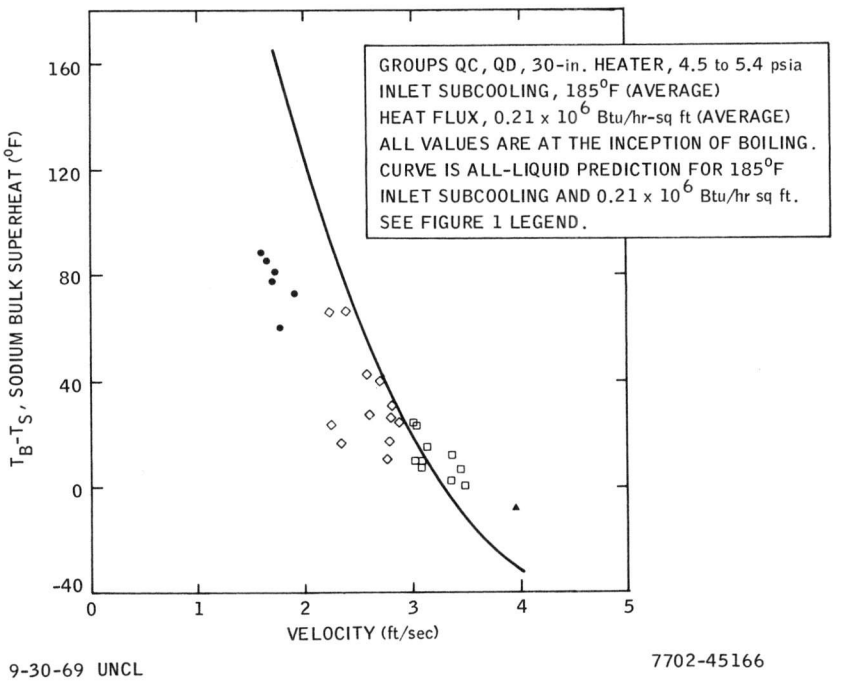

Figure 2. Sodium Bulk Superheat vs Sodium Velocity for Flow Coastdown Conditions

Bulk superheat is seen to decrease with increasing velocity, thereby corroborating the identical trend (superheat vs velocity) for potassium shown by Chen.* Comparison of the data trend with that obtained from all-liquid heat transfer considerations shows good agreement; the largest discrepancy occurring at the lowest velocity.

Typical fluid temperature, pressure, and flow traces are shown in Figure 3 for a flow coastdown run (Run QD-6). These runs are made by initially establishing pressure, inlet temperature, and flowrate, and then making a step change increase in heat input to the test section until a steady state higher fluid temperature is reached. The first portion of the temperature trace shows this event. With all conditions constant, the flow is then decreased gradually until boiling is initiated as detected by the boiling detectors.

*J. C. Chen, "Effect of Turbulent Flow on Incipient Boiling Superheat," Technical Working Group on Liquid-Metal Thermal Science Meeting, Brookhaven National Laboratory, May 22-23, 1969

SODIUM LIQUID SUPERHEAT TEST DATA
(Sheet 1 of 8)

Run No.[a]	Test Section Pressure (psia)	Test Section Inlet Temperature (°F)	Heat Flux $\left(\frac{\text{Btu/hr-ft}^2}{10^6}\right)$	Bulk Superheat (°F)	Wall[b] Superheat (°F)	Sodium Velocity (ft/sec)
PD-1[c]	4.77	1338	0.119	23	36	4.11
PD-2	4.78	1338	0.151	41	57	4.09
PD-3	4.97	1331	0.167	41	59	4.07
PD-4	5.22	1328	0.209	60	82	4.09
PD-5	4.82	1330	0.224	87	111	4.11
PD-6	4.79	1328	0.135	7	21	4.15
PD-7	4.79	1327	0.148	16	32	4.13
PD-8	4.79	1328	0.153	22	38	4.17
PD-9	4.78	1327	0.147	10	26	4.11
PD-10	4.78	1326	0.147	14	30	4.11
PD-11	4.79	1327	0.167	27	45	4.15
PD-12	5.00	1326	0.199	53	73	4.15
PD-13	4.94	1330	0.190	51	71	4.17
PD-14	4.88	1333	0.153	21	37	4.09
PD-15	4.98	1334	0.194	55	76	4.13
PD-16	4.92	1336	0.209	73	95	4.13
PD-17	4.89	1338	0.222	87	111	4.09
PD-18	5.00	1338	0.192	50	70	4.05
PD-19	4.94	1338	0.221	76	99	4.05
PD-20	4.95	1337	0.137	17	32	4.09
PD-21	4.86	1337	0.150	31	47	3.94
PD-22	5.00	1337	0.189	59	79	3.90
PD-23	4.83	1339	0.178	53	72	4.00
PD-24	4.81	1338	0.134	18	32	3.94
PD-25	4.97	1328	0.184	35	55	3.90
PD-26[d]	4.91	1328	0.141	8	23	4.09
PD-27	4.86	1335	0.158	19	36	4.13
PD-28	4.89	1335	0.174	40	58	4.11
PD-29	4.86	1333	0.161	24	41	4.15
PD-30	5.03	1330	0.208	58	78	4.13
PD-31	4.77	1326	0.224	85	109	4.11
PD-32	4.86	1325	0.212	70	92	4.09
PD-33	4.92	1327	0.243	99	125	4.11
PD-34	4.50	1331	0.166	28	45	4.11
PD-35	5.47	1333	0.251	81	108	4.11
PD-36	4.64	1335	0.236	105	130	4.09
PD-37	4.69	1337	0.241	113	138	4.07
PD-38	4.29	1336	0.117	29	41	4.00
PD-39	4.62	1338	0.240	107	132	4.07
PD-40	4.74	1335	0.253	109	136	4.05

SODIUM LIQUID SUPERHEAT TEST DATA
(Sheet 2 of 8))

Run No.[a]	Test Section Pressure (psia)	Test Section Inlet Temperature (°F)	Heat Flux $\left(\frac{\text{Btu/hr-ft}^2}{10^6}\right)$	Bulk Superheat (°F)	Wall[b] Superheat (°F)	Sodium Velocity (ft/sec)
PD-41	4.88	1331	0.271	115	144	4.07
PD-42	4.57	1328	0.207	68	90	4.15
PD-43	4.73	1329	0.268	114	142	4.09
PD-44	4.62	1330	0.243	90	116	4.11
PD-45	4.26	1331	0.127	27	40	4.11
PD-46	4.37	1331	0.171	51	69	4.11
PD-47	4.55	1332	0.247	101	127	4.11
PD-48	4.83	1334	0.269	116	144	4.11
PD-49	4.31	1334	0.114	25	37	4.13
PD-50	4.22	1333	0.117	20	32	4.11
PE-1[e]	5.09	1334	0.170	44	62	3.05
PE-2	4.95	1331	0.190	69	89	3.03
PE-3	4.90	1331	0.213	84	107	3.05
PE-4	4.90	1330	0.219	103	126	3.03
PE-5	4.92	1329	0.233	119	144	3.05
PE-6	4.94	1329	0.158	41	58	3.03
PE-7	4.82	1334	0.181	70	89	3.03
PE-8	4.98	1337	0.190	80	100	3.00
PE-9	5.02	1338	0.205	98	120	3.00
PE-10	5.07	1337	0.186	78	98	3.00
PE-11	5.10	1336	0.211	92	112	3.03
PE-12	5.02	1336	0.209	100	122	3.00
PE-13	5.00	1334	0.150	34	50	3.00
PE-14	4.90	1335	0.143	35	50	3.05
PE-15	4.88	1336	0.178	71	90	3.05
PE-16	5.00	1336	0.194	81	102	3.00
PE-17	5.01	1335	0.200	86	107	2.98
PE-18	5.03	1334	0.184	66	86	2.98
PE-19	4.97	1331	0.175	69	88	3.00
PE-20	5.00	1331	0.212	87	109	3.05
PE-21	4.98	1330	0.206	93	115	3.03
PE-22	4.92	1329	0.131	16	30	3.03
PE-23	4.93	1329	0.159	35	52	3.07
PE-24	5.01	1330	0.204	77	99	3.07
PE-25	5.04	1334	0.214	101	124	3.03
PE-26[f]	5.10	1334	0.178	44	63	3.05
PE-27	4.92	1334	0.178	59	78	3.05
PE-28	5.10	1334	0.194	76	97	3.05
PE-29	5.01	1333	0.222	96	120	3.05
PE-30	5.15	1332	0.222	98	122	3.05

SODIUM LIQUID SUPERHEAT TEST DATA
(Sheet 3 of 8)

Run No.[a]	Test Section Pressure (psia)	Test Section Inlet Temperature (°F)	Heat Flux $\left(\frac{\text{Btu/hr-ft}^2}{10^6}\right)$	Bulk Superheat (°F)	Wall[b] Superheat (°F)	Sodium Velocity (ft/sec)
PE-31	4.98	1332	0.185	55	75	3.03
PE-32	5.10	1333	0.225	96	120	3.03
PE-33	5.30	1334	0.251	130	157	3.07
PE-34	5.32	1332	0.202	76	98	3.00
PE-35	5.30	1333	0.245	120	146	3.00
PE-36	5.29	1332	0.220	86	110	3.00
PE-37	5.04	1333	0.118	12	26	2.98
PE-38	4.95	1333	0.149	34	50	3.09
PE-39	4.80	1328	0.189	66	86	3.09
PE-40	4.81	1325	0.146	29	44	3.07
PE-41	4.78	1325	0.135	27	41	3.05
PE-42	4.76	1323	0.137	23	37	2.96
PE-43	4.74	1326	0.163	50	67	3.05
PE-44	4.83	1328	0.177	54	73	3.05
PE-45	4.91	1330	0.190	69	89	3.09
PE-46	4.89	1330	0.149	42	58	3.03
PE-47	4.83	1331	0.136	25	39	3.00
PE-48	4.76	1333	0.123	19	32	3.03
PE-49	4.85	1333	0.156	46	63	3.00
PE-50	4.84	1334	0.180	70	89	3.03
PF-1[g]	4.95	1232	0.226	-8	16	4.05
PF-2	4.94	1233	0.228	-12	12	4.05
PF-3	4.93	1232	0.231	-3	21	4.03
PF-4	4.92	1232	0.209	-26	-4	3.98
PF-5	4.94	1234	0.252	14	41	4.00
PF-6	4.81	1235	0.239	7	32	4.03
PF-7	4.90	1237	0.242	7	33	4.05
PF-8	4.95	1239	0.227	1	25	3.98
PF-9	4.91	1242	0.229	-7	17	3.98
PF-10	4.92	1242	0.222	-9	14	4.03
PF-11	4.93	1242	0.244	6	32	4.07
PF-12	4.95	1240	0.229	-7	17	4.03
PF-13	4.95	1239	0.229	-1	23	3.98
PF-14	4.95	1238	0.232	-7	18	4.07
PF-15	4.95	1237	0.231	-13	11	3.98
PF-16	4.95	1236	0.236	-14	11	4.09
PF-17	4.95	1235	0.235	-5	20	4.05
PF-18	4.89	1237	0.234	1	26	4.03
PF-19	4.91	1237	0.223	-12	12	4.05
PF-20	4.92	1236	0.238	-5	20	4.03

SODIUM LIQUID SUPERHEAT TEST DATA
(Sheet 4 of 8)

Run No.[a]	Test Section Pressure (psia)	Test Section Inlet Temperature (°F)	Heat Flux $\left(\frac{\text{Btu/hr-ft}^2}{10^6}\right)$	Bulk Superheat (°F)	Wall[b] Superheat (°F)	Sodium Velocity (ft/sec)
PF-21	4.92	1236	0.235	-11	14	3.98
PF-22	4.92	1235	0.240	0	25	4.05
PF-23	4.92	1234	0.243	-6	20	4.03
PF-24	4.92	1234	0.249	17	43	3.98
PF-25	4.97	1235	0.248	14	40	4.03
PF-26[h]	4.89	1236	0.250	-6	20	4.05
PF-27	4.91	1237	0.258	3	24	4.05
PF-28	4.92	1236	0.258	0	27	4.09
PF-29	4.92	1236	0.251	0	26	4.15
PF-30	4.92	1238	0.251	-5	21	3.94
PF-31	4.92	1239	0.252	-2	25	4.03
PF-32	4.91	1234	0.261	-6	22	4.09
PF-33	4.91	1235	0.252	-7	20	4.03
PF-34	4.91	1237	0.247	-5	21	3.98
PF-35	4.92	1237	0.257	-6	21	3.96
PF-36	4.92	1238	0.255	-5	22	4.03
PF-37	4.92	1236	0.255	-1	26	4.11
PF-38	4.94	1236	0.259	-7	20	4.07
PF-39	4.94	1235	0.253	-14	13	4.07
PF-40	4.94	1234	0.262	1	29	4.09
PF-41	4.95	1237	0.265	-1	27	4.03
PF-42	4.95	1239	0.257	-4	23	4.11
PF-43	4.94	1236	0.258	-7	20	4.11
PF-44	4.94	1236	0.260	-4	23	4.05
PF-45	4.96	1236	0.272	1	30	4.03
PF-46	4.97	1235	0.265	-6	22	4.09
PF-47	4.96	1235	0.255	-6	21	4.13
PF-48	4.96	1235	0.270	-3	26	4.07
PF-49	4.97	1234	0.258	7	20	4.11
PF-50	4.96	1236	0.251	-9	18	4.07
QA-1[j]	5.07	1234	0.251	-6	21	4.15
QA-2	5.23	1234	0.308	43	76	4.17
QA-3	4.82	1235	0.265	9	37	4.20
QA-4	4.91	1234	0.264	-4	24	4.15
QA-5	4.92	1235	0.259	-2	25	4.20
QA-6	5.49	1236	0.336	54	90	4.15
QA-7	5.03	1239	0.272	4	33	4.15
QA-8	5.21	1242	0.323	50	84	4.02
QA-9	5.20	1238	0.303	15	47	4.09
QA-10	5.37	1233	0.341	6	42	4.07

SODIUM LIQUID SUPERHEAT TEST DATA
(Sheet 5 of 8)

Run No.[a]	Test Section Pressure (psia)	Test Section Inlet Temperature (°F)	Heat Flux $\left(\frac{\text{Btu/hr-ft}^2}{10^6}\right)$	Bulk Superheat (°F)	Wall[b] Superheat (°F)	Sodium Velocity (ft/sec)
QA-11	5.01	1231	0.272	-6	23	4.05
QA-12	5.20	1231	0.319	8	41	4.11
QA-13	5.17	1233	0.322	6	40	4.09
QA-14	4.95	1234	0.312	21	54	4.07
QA-15	4.83	1239	0.286	11	41	4.09
QA-16	4.91	1236	0.289	10	41	4.05
QA-17	4.91	1231	0.283	5	35	4.05
QA-18	5.14	1231	0.330	27	62	4.00
QA-19	5.04	1230	0.326	10	45	4.03
QA-20	5.10	1231	0.345	24	61	4.07
QA-21	5.20	1232	0.330	30	65	4.07
QA-22	5.30	1234	0.327	22	57	4.09
QA-23	5.10	1235	0.321	26	60	4.09
QA-24	5.15	1237	0.329	10	45	4.07
QA-25	5.10	1236	0.322	14	48	4.05
QA-26[k]	5.10	1233	0.280	28	58	3.05
QA-27	4.86	1233	0.229	10	34	3.07
QA-28	5.00	1231	0.252	30	57	3.09
QA-29	5.07	1231	0.278	30	60	3.05
QA-30	5.01	1231	0.266	49	77	3.07
QA-31	5.25	1232	0.333	111	146	3.11
QA-32	5.30	1233	0.289	65	96	3.05
QA-33	5.21	1234	0.295	86	117	3.09
QA-34	5.14	1235	0.275	69	98	3.11
QA-35	4.89	1235	0.304	87	119	3.11
QA-36	4.98	1231	0.283	74	104	3.05
QA-37	5.01	1229	0.314	101	134	3.09
QA-38	5.19	1227	0.331	118	153	3.07
QA-39	5.16	1226	0.323	97	131	3.09
QA-40	5.12	1226	0.329	102	137	3.09
QA-41	5.15	1226	0.344	120	157	3.09
QA-42	5.31	1228	0.352	132	169	3.13
QA-43	5.10	1229	0.299	79	111	3.11
QA-44	4.82	1231	0.268	59	87	3.09
QA-45	5.01	1233	0.306	93	126	3.02
QA-46	5.01	1235	0.240	29	55	3.09
QA-47	4.83	1235	0.251	43	70	3.05
QA-48	4.90	1235	0.248	45	71	3.07
QA-49	5.10	1235	0.246	33	59	3.05
QA-50	5.03	1236	0.288	81	112	3.00

SODIUM LIQUID SUPERHEAT TEST DATA
(Sheet 6 of 8)

Run No.[a]	Test Section Pressure (psia)	Test Section Inlet Temperature (°F)	Heat Flux $\left(\frac{\text{Btu/hr-ft}^2}{10^6}\right)$	Bulk Superheat (°F)	Wall[b] Superheat (°F)	Sodium Velocity (ft/sec)
QB-1[l]	4.88	1236	0.341	1	37	6.07
QB-2	4.78	1233	0.345	-8	28	6.13
QB-3	5.14	1233	0.381	-2	38	6.11
QB-4	4.83	1233	0.354	-5	32	6.18
QB-5	4.97	1237	0.366	-2	37	6.07
QB-6	4.98	1240	0.353	-11	26	6.13
QB-7	5.15	1242	0.370	-2	37	6.13
QB-8	4.89	1235	0.357	-11	26	6.07
QB-9	4.95	1236	0.367	-8	31	6.13
QB-10	4.97	1236	0.377	-6	35	6.18
QB-11	5.04	1236	0.388	4	45	6.09
QB-12	5.01	1237	0.365	-7	31	6.09
QB-13	4.93	1239	0.352	-9	28	6.22
QB-14	4.93	1238	0.352	-8	29	6.11
QB-15	5.01	1235	0.360	-7	31	6.13
QB-16	5.07	1235	0.383	-3	37	6.11
QB-17	4.93	1238	0.352	-8	29	6.09
QB-18	5.06	1237	0.386	3	44	6.07
QB-19	4.97	1233	0.373	-2	37	6.07
QB-20	4.91	1239	0.352	-7	34	6.11
QB-21	5.12	1236	0.389	-4	37	6.09
QB-22	5.04	1233	0.389	-2	39	6.16
QB-23	4.98	1233	0.366	-6	32	6.16
QB-24	4.90	1236	0.363	-5	33	6.13
QB-25	4.97	1238	0.369	-3	36	6.11
QB-26[m]	5.22	1233	0.506	-29	24	8.88
QB-27	5.24	1231	0.474	-15	34	8.86
QB-28	5.15	1237	0.477	-18	32	8.84
QB-29	5.13	1232	0.479	-25	25	8.90
QB-30	5.13	1236	0.477	-17	33	8.86
QB-31	5.15	1238	0.469	-19	30	8.80
QB-32	5.13	1231	0.488	-20	1	8.84
QB-33	5.23	1234	0.516	-16	18	8.84
QB-34	5.22	1236	0.485	-19	32	8.92
QB-35	5.19	1236	0.496	-20	32	8.90
QB-36	5.20	1235	0.481	-17	33	8.90
QB-37	5.22	1236	0.494	-16	36	8.80
QB-38	5.19	1234	0.482	-18	33	8.88
QB-39	5.26	1236	0.473	-20	29	8.88
QB-40	5.21	1236	0.496	-15	37	8.80

SODIUM LIQUID SUPERHEAT TEST DATA
(Sheet 7 of 8)

Run No.[a]	Test Section Pressure (psia)	Test Section Inlet Temperature (°F)	Heat Flux $\left(\frac{\text{Btu/hr-ft}^2}{10^6}\right)$	Bulk Superheat (°F)	Wall[b] Superheat (°F)	Sodium Velocity (ft/sec)
QB-41	5.20	1231	0.499	-15	37	8.84
QB-42	5.19	1234	0.491	-14	37	8.92
QB-43	5.28	1234	0.501	-17	36	8.80
QB-44	5.21	1233	0.483	-19	32	8.86
QB-45	5.19	1234	0.510	-17	37	8.82
QB-46	5.22	1234	0.492	-18	33	8.80
QB-47	5.22	1232	0.513	-19	35	8.78
QB-48	5.28	1238	0.544	-13	44	8.88
QB-49	5.31	1230	0.537	-18	38	8.90
QB-50	5.30	1232	0.528	-18	37	8.92
QC-1[n]	5.19	1234	0.248	14	40	3.15
QC-2	5.36	1240	0.224	16	40	2.34
QC-3	5.01	1247	0.218	39	62	2.73
QC-4	5.03	1236	0.218	10	33	2.77
QC-5	4.80	1236	0.223	26	50	2.79
QC-6	4.68	1233	0.218	10	33	3.09
QC-7	4.95	1238	0.221	23	46	2.24
QC-8	5.00	1237	0.218	85	108	1.66
QC-9	4.87	1239	0.218	30	53	2.81
QC-10	4.79	1238	0.220	2	25	3.34
QC-11	4.47	1235	0.204	11	33	3.37
QC-12	4.78	1233	0.215	66	89	2.39
QC-13	4.62	1233	0.212	22	44	3.02
QC-14	4.62	1233	0.188	27	47	2.62
QC-15	4.62	1234	0.201	17	38	2.79
QC-16	4.63	1238	0.201	23	44	2.98
QC-17	4.62	1237	0.199	8	29	3.09
QC-18	4.62	1236	0.200	0	21	3.45
QC-19	4.62	1235	0.203	0	21	3.49
QC-20	4.62	1236	0.203	6	27	3.44
QC-21	4.58	1132	0.315	-6	27	3.30
QC-22	4.59	1126	0.310	-10	22	2.98
QC-23	4.59	1127	0.320	-10	22	3.09
QC-24	4.59	1136	0.319	-7	27	3.45
QC-25	4.61	1136	0.316	-7	26	3.24
QC-26	4.59	1131	0.323	-6	28	3.30
QC-27	4.59	1131	0.329	0	35	3.22
QC-28	4.61	1132	0.330	-7	28	3.32
QC-29	4.60	1133	0.327	-8	26	3.41
QC-30	4.61	1135	0.327	-6	28	3.22

SODIUM LIQUID SUPERHEAT TEST DATA
(Sheet 8 of 8)

Run No.[a]	Test Section Pressure (psia)	Test Section Inlet Temperature (°F)	Heat Flux $\left(\frac{\text{Btu/hr-ft}^2}{10^6}\right)$	Bulk Superheat (°F)	Wall[b] Superheat (°F)	Sodium Velocity (ft/sec)
QD-1[p]	4.78	1238	0.221	42	65	2.58
QD-2	4.77	1240	0.218	24	47	2.88
QD-3	4.68	1232	0.218	88	101	1.62
QD-4	4.71	1217	0.215	59	82	1.79
QD-5	4.89	1225	0.218	65	88	2.24
QD-6	5.06	1231	0.220	72	95	1.92
QD-7	4.73	1240	0.218	-9	14	3.96
QD-8	4.90	1239	0.212	77	100	1.70
QD-9	5.07	1233	0.216	81	104	1.73
QD-10	4.80	1234	0.214	9	32	3.05
QD-11	5.09	1021	0.417	14	58	2.58
QD-12	5.19	1025	0.421	42	87	2.39
QD-13	5.06	1035	0.424	8	53	3.05
QD-14	5.04	1032	0.423	11	56	2.98
QD-15	5.04	1036	0.423	-10	35	3.34
QD-16	5.06	1037	0.427	3	48	3.02
QD-17	5.06	1037	0.427	-4	41	3.30
QD-18	5.07	1036	0.424	0	45	3.26
QD-19	5.01	1034	0.427	1	46	3.41
QD-20	5.10	1036	0.429	3	48	3.21

(a) The condenser cover-gas pressure is 5 psia for each run.
(b) These values are the summation of the bulk superheat plus a calculated film drop obtained by using equations from W. M. Kays et al., "Heat Transfer in Annular Passages - Hydrodynamically Developed Turbulent Flow with Arbitrarily Prescribed Heat Flux," International Journal of Heat and Mass Transfer, Vol. 6, p 537 (1963).
(c) Maximum pressure = 5 psia held for 24 hr
(d) Maximum pressure = 5 psia held for 24 hr
(e) Maximum pressure = 6 psia held for 24 hr
(f) Maximum pressure = 5 psia held for 24 hr
(g) Maximum pressure = 10 psia held for 24 hr
(h) Maximum pressure = 7 psia held for 24 hr
(j) Maximum pressure = 9 psia held for 24 hr
(k) Maximum pressure = 5 psia held for 24 hr
(l) Maximum pressure = 5 psia held for 24 hr
(m) Maximum pressure = 5 psia held for 24 hr
(n) Maximum pressure = 10 psia held for 24 hr
(p) Maximum pressure = 10 psia held for 18 hr

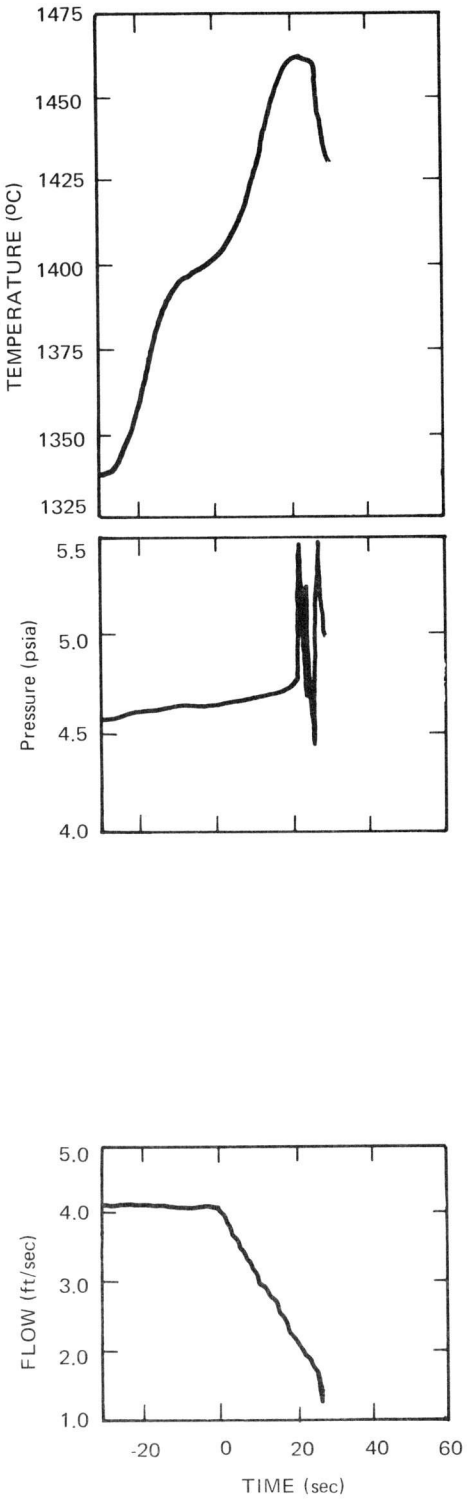

Figure 3. Typical Data for a Flow Coastdown Run

B. PHASE I TOPICAL REPORT ON SINGLE CHANNEL SUPERHEATING

A topical report, "Studies of Boiling Initiation for Sodium Flowing in a Heated Channel," AI-AEC-12767, is presently being reviewed for patent clearance prior to publication.

A summary of the contents of the topical report was presented in the Annual Technical Progress Report GFY 1969, AI-AEC-12860.

C. HEATER DEVELOPMENT

A 30-in. shaped flux heater was developed, fabricated, and tested to a heat flux of 10^6 Btu/hr-ft^2. The heating element was constructed from short pieces of hollow graphite. By appropriately varying the cross-sectional area of each graphite piece, a controlled axial heat flux profile was produced.

D. THREE-CHANNEL TEST SECTION

A three channel test section insert has been fabricated and instrumented. The insert is ready for installation into the loop and will accommodate a 15-in. three-pin heater. The clover leaf shape of the flow channel was designed to equalize the flow per heater for each 60° arc of heater.

The three-pin heater components have been fabricated, and the heater is ready to be assembled. The pitch-to-diameter ratio of the pins has been maintained at 1.487, the same as for the FFTF fuel pins.

IV. EVALUATION OF EFFORT TO DATE

The progress is considered to be satisfactory. Three hundred and seventy-four liquid superheat tests were performed this quarter. The three-channel test section flow distributor insert has been fabricated and instrumented. A 30-in. shaped flux heater was fabricated and tested to a heat flux of 10^6 Btu/hr-ft^2.

V. NEXT REPORT PERIOD ACTIVITIES

The three-channel test section will be installed, and three-channel experimentation will be started.

The topical report on the early single channel liquid superheat work will be released as AI-AEC-12767.

The topical report on the multichannel, boiling-sodium code, SODIFAZE, will be completed.

Blank Page

Program:	HNPF
AEC Task:	Task 13, HNPF Retirement
Project Manager:	B. F. Ureda
Reporting Period:	Fiscal Year 1969
General Order:	7709
Subaccount:	All
AEC Category:	82-01-02-03.0

Principal Investigator: B. F. Ureda

I. PROJECT OBJECTIVES

The objective of this project is to provide technological support to the AEC and Consumers Public Power District and to provide documentation of the conduct of the work. During the past quarter specific tasks were as follows.

a) Continued on-site surveillance of the demolition contractors' activities in disposing of the reactor building, warehouse, calibration building, and moderator assembly building; and the property in these buildings.

b) Reviewing modifications to the designs of the final cover over the isolation structure and monitoring the progress of the construction of this cover.

c) Reviewing the comments made by CPPD on the Final Safety Report and issuing a revision of the report.

d) Preparing the HNPF Retirement Program Final Summary Report and preparing the Motion Picture Record of the principal activities of the retirement.

e) Keeping a current record of program costs and issuing a monthly statement.

II. MAJOR ACCOMPLISHMENTS DURING FISCAL YEAR 1970

The major accomplishments during the first quarter of fiscal year 1970 were as follows.

a) The demolition contractor completed his work of removal of the HNPF buildings and area cleanup on August 25, 1969.

b) The placement of the final cover over the isolation structure was completed on September 16, 1969.

c) The Final Safety Report and Final Summary Report were revised and readied for release. The final footage for the Motion Picture film was taken.

III. PROGRESS REPORT DURING REPORT PERIOD

The demolition contractor left the site on August 25, 1969. His work originally was scheduled to be completed on April 15, 1969. The labor problems, severe weather, and equipment failures contributed adversely to his progress. The delay in the demolition work caused a several weeks delay in the initiation and progress of the placement of the final cover over the isolation structure. The demolition contractor did an exceptionally complete job in his final cleanup; picking up and disposing of scrap materials down to nut and bolt size.

Placement of the final protective cover over the isolation structure began slowly because of interference with the demolition work. However, by late July, the crew size was up to 50 people. Several work stoppages occurred because of jurisdictional labor difficulties and heavy rains. The schedule set out by the contractor prior to beginning the work was missed by two weeks. The work was completed on September 16, 1969. The attached photograph shows the HNPF site in its final retired configuration.

Reporting on the site activities continued throughout the period. CPPD submitted their comments on the Safety Analysis Report, and these comments have been incorporated into a revision as applicable. The final Summary Report has been reviewed internally at Atomics International. A revision of the report is being readied for printing. Final footage for the motion picture film was taken in September. A film record of the placement of the isolation structure protective cover and the final environmental survey were taken earlier in the period.

Atomics International has closed its offices at Hallam, discontinuing full-time site coverage by representatives.

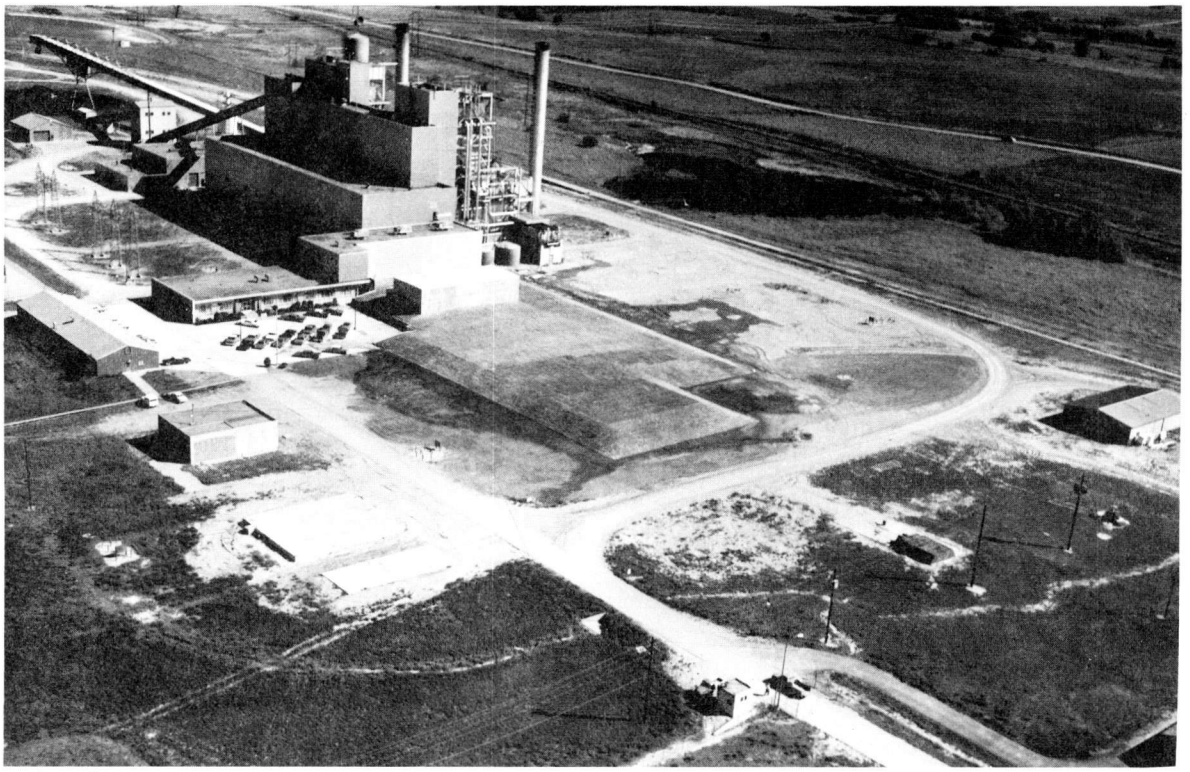

9/18/69 7709-10163

Configuration of Retired Hallam Nuclear Power Facility Site

IV. EVALUATION OF EFFORT TO DATE

The physical efforts at the HNPF site are completed. The delays may have been avoided if better cooperation from the construction unions had been possible. Labor difficulties and weather plagued the entire effort. However, the work is finished; and the visible end product has a pleasant, serene appearance satisfactory to all concerned.

V. NEXT REPORT PERIOD ACTIVITIES

The next report period activities will center around finalizing the program documentation. The three documents: "Final Status Report and Safety Analysis of the HNPF Site and Remaining Structures; HNPF Retirement Program Summary; and the HNPF Retirement Motion Picture" will be released for final approvals and will be revised if necessary.

The plaque to be installed in the IHX wall at the site will be engraved and shipped to the site as soon as acceptable wording is established by the AEC contracting officer's office.

Program:	Advanced Development Program	
AEC Task:	15, High Temperature Chemistry	
Project Manager:	S. J. Yosim	
Reporting Period:	July-September 1969	
General Order: 7711	Subaccount: 53020	AEC Category: 05-05-01-00.0

I. PROJECT OBJECTIVES

This project is divided into two general areas; namely, the study of fused salts and the study of metal-metal salt solutions. The objective of the study of fused salts is to achieve an understanding of ionic melts (halides, oxides, oxy-salts, and glass systems) by (a) establishing the nature of the species existing in ionic melts, (b) determining the physico-chemical interactions between species, and (c) formulating systematic relationships between the physico-chemical properties of fused salt systems and the molecular parameters of the species.

The objectives of the metal-metal salt study are to determine phase diagrams for, and the nature of interactions between metals and their salts at high temperatures, to determine the species in these solutions, and, finally, to predict the solubilities in metal salt systems.

II. MAJOR ACCOMPLISHMENTS IN FISCAL YEAR 1970

A. PAPERS PUBLISHED

1. "Electronic Conduction in Fused Salts," by L. F. Grantham and S. J. Yosim in "Molten Salts — Characterization and Analysis," Ed. by Gleb Mamantov, published by Marcel Dekker, Inc. 1969
2. "Some Fundamental Concepts in the Chemistry of Molten Salts," by Milton Blander in "Molten Salts — Characterization and Analysis," Ed. by Gleb Mamantov — published by Marcel Dekker, Inc. 1969

B. PAPERS IN PRESS

3. "A Redetermination of the Thermoelectric Properties of the Bi-$BiBr_3$ System," by J. D. Kellner, S. J. Yosim, and L. E. Topol, J. Phys. Chem

4. "Thermodynamics of the Fm3m ⇄ Pm3m Transition in the Potassium and Rubidium Halides," by A. J. Darnell and W. A. McCollum, in Journal of Physics and Chemistry of Solids

5. "The Electrical Conductivity of Aluminum Chloride Liquid and Supercritical Vapor," by C. R. Boston, S. J. Yosim, and L. F. Grantham, J. Chem. Phys.

6. "Electrical Conductivities of Molten Aluminum Chloride-Potassium Chloride Mixtures," by C. R. Boston, L. F. Grantham, and S. J. Yosim in J. Electrochem. Soc.

7. "The Electrical Conductivities of Molten $BiCl_3$, $BiBr_3$, and BiI_3 at High Pressure," by A. J. Darnell, W. A. McCollum, and S. J. Yosim in J. Phys. Chem.

III. PROGRESS DURING REPORT PERIOD

In an earlier company-funded program it was noted in one experiment that water "quenched" from high pressures and temperatures showed a lower vapor pressure than normal water. It is possible that this "quenched" water could be of the same molecular form as the recently reported anomalous or polymerized water reported by Deryagin (1964) and Lippincott (1969). Large differences in the dielectric constant between these two forms would be expected. Preliminary bench top mockup tests have been made on an apparatus to measure the dielectric constant of water at extreme pressures as a possible tool in examining this phenomenon.

IV. EVALUATION OF EFFORT TO DATE

The emphasis in the experimental approach will continue on high pressure and transport experiments.

V. NEXT REPORT PERIOD ACTIVITIES

The dielectric constant of water will be measured to 25 kilobars at temperatures to 150°C. Attempts will be made to prepare anomalous water by using high pressure-high temperature techniques.

Program:	Physical Research Program
AEC Task:	17, Electronic Structure of Metals and Alloys
Project Manager:	R. G. Breckenridge
Reporting Period:	July-September 1969
General Order: 7713	Subaccount: 54010 AEC Category: 05-06-02-00.0

Principal Scientists: R. G. Breckenridge, L. J. Barnes, H. J. Fink, S. L. Wipf, and M. M. Nakata

I. PROJECT OBJECTIVES

This effort is devoted to the acquisition of knowledge regarding the electronic structure of metals and alloys (configuration of electronic energy states in momentum space) and the role of this structure in determining electrical, thermal, magnetic, vibrational, and alloying characteristics. Detailed information on the shape of the Fermi surface is provided by de Haas-van Alphen studies in magnetic fields up to 200 kilogauss, and the density of electronic states at the Fermi level is deduced from low-temperature specific heat measurements. The latter also yield information on lattice vibrational modes and on the interactions involved in superconductivity and magnet ordering. Further characterization of magnetic interactions is accomplished by means of conventional magnetic susceptibility techniques. Considerable effort is devoted to the exploration of high field superconductivity with emphasis on thermodynamic and transport characteristics, as well as on the electron energy spectrum as deduced from point contact tunneling measurements. These experimental investigations are correlated with current theory, and attempts are made to characterize quantitatively the relationship between superconductivity and the normal-state electronic structure.

II. MAJOR ACCOMPLISHMENTS IN FISCAL YEAR 1970

Publications were as follows.

1. H. J. Fink and A. G. Presson, "Stability Limit of the Superheated Meissner State due to Three Dimensional Fluctuations of the Order Parameter and Vector Potential," Phys. Rev. 182, 498 (1969)

2. H. J. Fink and W.C. H. Joiner, "Surface Nucleation and Boundary Conditions in Superconductors," Phys. Rev. Letters 23, 120 (1969)

3. H. J. Fink and A. G. Presson, "Proximity Effect of Superconductors in High Magnetic Fields," Phys. Rev., accepted for publication

4. H. J. Fink and A. G. Presson, "Superconducting Surface Sheath of a Semi-Infinite Half Space and its Instability Due to Fluctuations," submitted to Phys. Rev.

III. TECHNICAL PROGRESS DURING REPORT PERIOD

A. STABILITY LIMIT OF THE SUPERHEATED MEISSNER STATE DUE TO THREE DIMENSIONAL FLUCTUATIONS OF THE ORDER PARAMETER AND VECTOR POTENTIAL, H. J. Fink

We have calculated near the transition temperature T_c the upper experimental magnetic field H_u at which the metastable, superheated Meissner state becomes unstable against infinitesimally small fluctuation of the order parameter and the vector potential. For $\kappa \leq 1.10$, the stability limit is determined by fluctuations of infinite wave length, and the field H_u coincides with the maximum field H_{sh} at which solutions of the Ginzburg-Landau equations cease to exist. For $\kappa > 1.10$, the value of $H_u < H_{sh}$. For example, at $\kappa \approx 4.25$, the value of $H_u/H_c \approx 1$; and when $\kappa \to \infty$, the value of $H_u/H_c \approx 0.745$ (H_c is the thermodynamic critical field). For $\kappa \geq 1.10$, one finds within one percent $H_u/H_c = (\sqrt{5/3})(1 + 1/\sqrt{2\kappa})$.

B. SURFACE NUCLEATION AND BOUNDARY CONDITIONS IN SUPERCONDUCTORS, H. J. Fink

We have calculated the surface nucleation field as a function of the slope of the superconducting order parameter at the surface of a semi-infinite superconducting half-space. When the order parameter increases on approaching the surface, as would be the case in the presence of a surface region of enhanced transition temperature, nucleation fields larger than those expected for a uniform sample are predicted. Cold working the surface on an InBi foil produces this condition and qualitatively confirms the prediction.

C. SUPERCONDUCTING SURFACE SHEATH OF A SEMI-INFINITE HALF SPACE AND ITS INSTABILITY DUE TO FLUCTUATIONS, H. J. Fink

The surface sheath of a semi-infinite half space for applied magnetic fields $H_o \geq H_{c2}$ and Ginsburg Landau $\varkappa$ values ≥ 0.707 was investigated with regard to its current-carrying capacity and stability. It is found that infinitesimally three-dimensional fluctuations of the order parameter and the vector potential make the surface sheath unstable and the total stable transport current zero.

D. PROXIMITY EFFECT OF SUPERCONDUCTORS IN HIGH MAGNETIC FIELDS, H. J. Fink

The nucleation field H_o for superconductivity at the boundary between a normal and a superconducting semi-infinite half space is calculated. At this field, for temperatures smaller than the transition temperature T_{cs} of the superconductor, a second-order phase transition occurs from the normal to the superconducting state as the magnetic field is decreased, and superconductivity is nucleated near the boundary between the superconducting and the normal metal. The calculation is general and is applied to clean and dirty superconductors. The normal metal becomes also a superconductor at a transition temperature $T_{cm} < T_{cs}$, and the above results apply to temperatures $T_{cn} \leq T \leq T_{cs}$ as well as $T < T_{cn}$, provided the Ginzburg-Landau equations apply. H_o is temperature-dependent, and lies between the bulk nucleation field H_{c2} and the surface nucleation field H_{c3}. The value of H_o depends on the BCS coherence lengths, ξ_o, the mean free paths ℓ in the normal states, the effective masses m, the electron densities n, and the transition temperatures T_c of both metals. For example, one finds, in the limit when both metals are dirty ($\ell \ll \xi_o$), that $H_{c2} \leq H_o \leq H_{c3}$ for $0 \leq \sigma_s/\sigma_n \leq \infty$, where the σ's are the normal-state conductivities of the superconducting and the normal metal. This is not in agreement with previous calculations by Hurault, who concludes that when $\sigma_s/\sigma_n = 1$, the value of H_o is H_{c2} for $T_{cn} \leq T \leq T_{cs}$. When $T < T_{cn}$, the value H_o is strongly field- and temperature-dependent, particularly when $\sigma_s/\sigma_n \lesssim 1$. The above concept is application to internal boundary nucleation of superconductivity in the bulk of a superconductor.

E. MEASUREMENT OF THERMODYNAMIC PROPERTIES WITH SUPERCONDUCTING WEAK LINKS, L. J. Barnes

An interesting possible method of measuring directly some thermodynamic properties of a superconductor involves measuring the free energy difference ΔF produced by a temperature difference ΔT. One would, ideally, be able to measure directly the electronic entropy of superconducting metals and alloys $S_e \alpha \Delta F/\Delta T$. The expected effect is extremely small ($\Delta T \sim 1°K \rightarrow \Delta F \sim 10^{-8}$ volts); and for all the usual techniques, it is completely impractical to attempt measurements. The A. C. Josephson effect at a superconducting weak link can in principal detect very small free energy differences; however, for frequencies below ~1 MHz, the effect is impossible to observe directly. The Ford group (Zimmerman, Silver, etc.), has shown that with the inclusion of a weak link (point contact) in a small superconducting or resistive ($\sim 10^{-6}\ \Omega$) loop with a small inductance ($<10^{-9}$ h) and the use of radio-frequency measuring techniques, the Josephson effect can be observed at frequencies as low as the cycles/sec range.

We have decided to try to use dynamic electrical properties of a small superconducting loop with one weak link in order to measure the expected temperature controlled free energy difference. The ideal and most convenient place to produce the free energy difference is at the weak link which is a point contact in our case. With this end in view, we have repeated the basic experiments, measuring the radio frequency properties of these loops. We have observed behavior essentially identical to that reported by the Ford group for both the superconducting and resistive loops. Flux quantization is observed as well as the Josephson effect due to voltage biasing a resistive shunt ($\sim 10^{-6}\ \Omega$). We can now proceed with some confidence of observing the thermal contact voltage we are looking for.

F. THERMAL PROPERTIES OF SUPERCONDUCTORS, M. M. Nakata

A program to measure the thermal diffusivity of selected superconductors below the critical temperature and, if possible, in a magnetic field has been started. In the method to be used, one face of a sample, which is in the form of a right circular cylinder, is irradiated with a short pulse of radiant energy.

The subsequent transient response of the opposite face is then related to the thermal diffusivity of the sample, according to the simple relation,

$$\alpha_{1/2} = 1.37a^2/\pi^2 t_{1/2}$$

where $t_{1/2}$ is the time required for the back face of the sample to reach half-maximum in its small temperature excursion and a is the sample thickness. Until now, this method has been used extensively at room temperature and above (>2000°C). The adaptation of the technique to cryogenic temperatures requires a number of changes in the design of the measuring equipment. The more important of these changes are in the light source, the temperature sensor, and the sample configuration. These design changes are necessitated due to heat loss considerations and gross changes in the physical properties of materials as they are cooled from ambient temperatures to liquid helium temperatures. Fabrication of a suitable thermometer with which to measure the temperature transient is also of vital importance.

The general design of the cryogenic thermal diffusivity apparatus has been completed and, with the exception of the sample holder and a few minor components, the construction of the apparatus has been essentially completed. Carbon thermometers are currently being fabricated, and these will be tested in a specially constructed holder, by using an auxiliary helium cryostat which has been set up for this purpose.

A knowledge of the thermal diffusivity is essential in order to calculate the occurrence of magnetic instabilities. It is also interesting to compare the data with existing specific heat and thermal conductivity measurements which are very few and unreliable. The thermal diffusivity is the ratio of specific heat and thermal conductivity but is easier to measure than either of these quantities.

Comparison with theories for short mean free path effects in superconductors are also expected to produce new insights. The superconductors to be investigated are mainly Nb-Ti alloys and also Nb-Zr. Pure Nb with well known specific heat and thermal conductivity may be used for testing and calibration.

IV. EVALUATION OF EFFORT DURING REPORT PERIOD

This report period has been a transitional one on the program since the operating level is being reduced for the coming fiscal year. In spite of this, substantial progress has been made on all of the project tasks. The theoretical work on superconductivity has produced some interesting results regarding the details of the nucleation of the superconducting state and the stability conditions of the surface sheath phase. Very good progress has been made on the measurements of the thermodynamic properties of superconducting properties using a point contact "weak link." The required electronic equipment for these very difficult measurements is now operating reliably. As a first step, some work reported from another laboratory has been reproduced, and now attention will turn to the proposed measurement of the electronic entropy in the superconductor. The third task, the study of the thermal diffusivity of superconductors has also progressed well. The apparatus for this rather elegant experiment is nearing completion and should be operating in the near future. This apparatus should generate a great deal of useful and valuable information.

V. EFFORTS PLANNED FOR NEXT QUARTER

The theoretical studies on this program are phasing out with the departure of Dr. Fink, but some work in progress will be completed in absentia. The experimental work on the weak links and thermal diffusivities will continue. The equipment for both studies should be in productive operation in this report period.

Program:	Physical Research Program	
AEC Task:	18, Radiation Damage in Crystalline Solids	
Project Manager:	R. G. Breckenridge	
Reporting Period:	July-September 1969	
General Order: 7714	Subaccount: 54040	AEC Category: 05-06-02-03.0

Principal Scientists: W. Bauer, D. W. Keefer, H. H. Neely, K. H. Thommen, D. D. Vawter, and A. Sosin

I. PROJECT OBJECTIVES

The materials requirements of modern technology demand an increased understanding of the effects of lattice defects on the physical properties of crystalline solids, and on their behavior when subjected to various kinds of radiation environments. Early recognition of the low thermal stability of some of the radiation-produced defects has resulted in emphasis on low temperature irradiation studies during the last 15 years. These investigations have elucidated many important aspects of defect production and defect properties, but concurrently have revealed the formidable complexity of radiation effects. While there remain still unanswered questions in the domain of low temperature radiation effects, the acquired insight now renders a study of radiation effects at higher temperatures a promising and desirable enterprise. It is the objective of this project to study the production of defects in crystalline solids by radiation, and to attain an understanding of their structure, their interactions with each other, and with impurities and dislocations. Low temperature electron irradiations are being used as an appropriate tool for the study of selected point defect problems in metals, metal alloys, and semiconductors. On the other hand, recognition of the realm of radiation damage at high temperatures and high particle fluxes as a relevant, but largely unexplored area, has made it desirable to expand the scope of this project. The program now includes investigation of phenomena unique to a high temperature, high flux radiation environment. Pure metals are chosen for this study because their use should lead to an improved understanding of the fundamental processes. This in turn should be helpful for the development of materials of superior properties.

II. MAJOR ACCOMPLISHMENTS DURING FISCAL YEAR 1970

Publications were as follows.

1) W. Bauer, K. Herschbach, and J. J. Jackson, "Low Temperature Electron and Alpha Particle Irradiation of Titanium," Phys. Rev. (to be published)

2) W. Bauer, A. Anderman, and A. Sosin, "Atomic Displacement Processes in Gold," Phys. Rev. (to be published)

3) K. Thommen, "Recovery of Low Temperature Electron-Irradiation-Induced Damage in n-type GaAs," submitted to "Radiation Effects"

III. PROGRESS DURING REPORT PERIOD

A. PROTON IRRADIATION OF NICKEL AT HIGH TEMPERATURES, K. Thommen, F. W. Eisen, and D. D. Vawter

Activities during this report period were mainly of a preparatory nature, but also included preliminary irradiations. Two sample holders for high temperature proton irradiation of nickel samples were completed and tested. Ten-mil nickel samples were prepared from 3-pass zone-refined nickel obtained from MRC. Removal of a $\sim$10,000 Å thick layer near the front face was practiced, by using an electrochemical etching technique. Two samples were irradiated with 400 kev protons at $\sim$500 and $\sim$600°C, respectively. The dose was 1×10^{18} protons/cm^2, averaged over a target area of 0.5 cm^2. These samples are presently being prepared for examination in the electron microscope. Various problems became apparent during these preliminary irradiations (1) The spacial irradiation intensity over the 0.5 cm^2 target area was not uniform; a possible remedy could be scanning of the beam, (2) The beam intensity could not be maintained at a constant value over long times (several hours); this appears to be an inherent shortcoming of the accelerator, at least if one has to run close to maximum beam intensity, (3) the maximum beam intensity was lower than expected; nevertheless, a dose of 1×10^{18} protons/cm^2 could be achieved within 5 hr, and (4) after the irradiation, it was found that the sample had become diffusion bonded to the copper parts between which it was sandwiched. This constitutes a serious difficulty and has induced us to

consider a modification of the sample mounting procedure which involves intentional diffusion bonding of a 0.5-mil thick nickel foil to a 50-mil thick copper plate. The copper plate will be dissolved in a two-stage process involving chemical and electrochemical etching. Both the diffusion bonding and the etching have been practiced, and satisfactory results have been achieved. With respect to the accelerator-related difficulties, we are considering the possibility of conducting irradiations with another accelerator.

B. SEMICONDUCTOR IRRADIATIONS — GaAs, K. Thommen and D. D. Vawter

Extensive isothermal annealing was performed for Stage I recovery at temperatures between 225 and 240°K, and for Stage II between 270 and 285°K. Within the experimental accuracy, recovery in both stages obeyed first order kinetics with the exception of a short initial period during the anneal at 225°K. The deviation from a simple exponential decay at 225°K is probably caused by a small unresolved recovery stage at the low temperature end of Stage I. The time constants of the exponential decay had a temperature dependence according to $\tau^{-1} = \nu_o e^{-E/kT}$ with $E = 0.72 \pm 0.04$ ev, $\nu_o = 10^{12.0 \pm 0.6}$ sec^{-1} for Stage I, and $E = 0.83 \pm 0.04$ ev, $\nu_o = 10^{11.6 \pm 0.6}$ sec^{-1} for Stage II. A first order process would be consistent with either recombination of closely spaced interstitials and vacancies under the influence of an attractive force, or long range migration of defects to sinks or deep traps. For the latter mechanism, the frequency factor depends on the sink or trap-concentration. In order to interpret either Stage I or Stage II recovery in terms of long range migration to sinks or traps, unreasonably large sink or trap concentrations such as 10^{15} dislocations per cm^2 or 10^{20} traps per cm^3 would have to be assumed. Therefore, long range migration can be excluded. For recombination of closely spaced interstitial vacancy pairs, one would expect a frequency factor of the order of $kT/h\nu$; i.e., $\sim 10^{13}$ sec^{-1} in our case. Our frequency factor values are somewhat lower, but not by an alarming amount. We suggest, therefore, that recovery in Stages I and II is due to recombination of closely spaced interstitials and vacancies. We wish to point out that this category of defect configurations is not necessarily restricted to single interstitial vacancy pairs. For instance, a divacancy with the two corresponding interstitials close to it, also could belong into this category. Under certain conditions, the annihilation of this type of defect by interstitial vacancy recombination also could obey first

order kinetics. A paper describing these and previously obtained recovery results has been submitted to "Radiation Effects" for publication.

III. PROGRESS DURING REPORT PERIOD

The main effort within this project has been devoted to necessary preparatory work for the high temperature proton irradiation studies in nickel. Valuable experience has been gained in sample preparation and handling techniques. Preliminary irradiations were very informative and suggested several desirable modifications of the experimental procedures.

Steady progress has been made in the study of electron irradiation-induced damage in GaAs. The results of the isothermal measurements permitted a more detailed interpretation of the low temperature recovery stages in this material.

IV. NEXT REPORT PERIOD ACTIVITIES

Emphasis will be on the proton irradiation studies of nickel. The experience gained in the preliminary irradiations will be used to perform future irradiations under improved conditions. Work on low temperature electron irradiation damage in GaAs will be continued on a reduced scale.

Program:	Advanced Development		
AEC Task:	22, Radiation Chemistry of Chromosomes		
Project Manager:	M. D. Sevilla		
Reporting Period:	July-September 1969		
General Order: 7724	Subaccount: 17001	AEC Category: 06-04-00-00.0	

I. PROJECT OBJECTIVES

The long-range objective of this study is to obtain information which will correlate molecular alterations with biological damage to mammalian chromosomes, caused by radiation. The immediate objective is a better understanding of the radiation chemistry of chromosomes and their main constituents, nucleic acids and proteins.

II. MAJOR ACCOMPLISHMENTS DURING FISCAL YEAR 1970

A. PUBLICATIONS AND PRESENTATIONS

1. Papers Accepted for Publication

a) "An Electron Spin Resonance Study of Acetate Dianion and Acetamide Anion," by M. D. Sevilla, J. Phys. Chem., December 1969

b) "The Reaction of Hydrogen Atoms with DNA," by R. A. Holroyd and J. W. Glass, Radiation Research, 1969

2. Papers Submitted for Publication

a) "An Electron Spin Resonance Study of Several Purine and Pyrimidine Anions," by M. D. Sevilla, submitted to J. Phys. Chem.

b) "Radicals Formed by the Reaction of Electrons with Amino Acids," by M. D. Sevilla, submitted to J. Phys. Chem.

3. Presentation Made

"Reactions of Electrons with Amino Acids and Dipeptides," M. D. Sevilla at the 158th National Meeting of the American Chem. Soc., September 9, 1969

B. TECHNICAL ACCOMPLISHMENTS

1) The study of the reactions of electrons with peptides was completed. The results showed that electron attachment to peptides results in the localization of the unpaired electron at the N-terminal peptide bond. The peptide anion is found to react by N-terminal deamination and the new species reacts further by abstraction. These results are considered most significant since they explain the mechanism of radiolysis of peptides. A paper describing these results is in preparation.

2) The study of the reaction of electrons with amino acids was completed. This study has shown that the electron initiates a series of radical-producing reactions upon attachment to amino acids. Each of the radicals produced was fully characterized. These results confirm that the electron is the most important radical-producing intermediate in the radiolysis of amino acids. A paper describing these results has been submitted for publication.

3) The ESR study of the acetate dianion and the acetamide anion was completed. Information concerning hyperfine splittings, the spin density distribution, and reactivities of these compounds was found. The acetate dianion results proved to be helpful in the analysis of the results of the amino acid dianions for which it served as a model compound. The acetamide anion results greatly aided the interpretation of the acetylpeptide anions. This resulted in the determination that electron localization occurs at the N-terminal peptide bond. A paper describing these results has been accepted for publication in J. Phys. Chem.

III. PROGRESS DURING REPORT PERIOD

A. REACTION OF ELECTRONS WITH DIPETIDES

The reactions of electrons with peptides in an alkaline glass were investigated as part of our study to determine the effects of radiolytic intermediates on constituents of chromosomes. Previous work on dipeptides (FY 1969) showed that electron attachment produces an anion which subsequently deaminates upon warming to form an N-terminal carbon radical. This radical species was then found to attack the parent compound by hydrogen abstraction to form a third radical species. This reaction scheme was found to be nearly identical to that

found for amino acids. Further, it suggested a mechanism (deamination from the N-terminal residue) which may be applicable to all peptides regardless of size. Several new dipeptides (glycyl-L-valine, glycyl-L-serine) have been recently investigated. They conform to the above mechanism. The work on dipeptides is completed. A paper is in preparation.

B. REACTIONS OF ELECTRONS WITH POLYPEPTIDES

In order to confirm the proposed mechanism for larger peptides the reaction of electrons with a tripeptide, L-alanylglycylglycine, and a pentapeptide, L-alanyl$(glycyl)_3$glycine were investigated. These compounds formed anions at low temperatures, which reacted upon warming to form radicals characteristic of a deamination from the N-terminal residue. The second radicals reacted to produce a third radical species by hydrogen abstraction from the glycyl residues. These results are in agreement with the proposed mechanism and suggest the mechanism may be extended to even larger peptides. This work is complete and a paper is in preparation.

C. REACTIONS OF ELECTRONS WITH ACETYL AMINO ACIDS AND ACETYL DIPEPTIDES

An N-terminal acetyl group removes the possibility of deamination of terminal amino (NH_2) groups in a peptide. Thus, the reaction of electrons with compounds with this group should determine whether C-N bond cleavage can occur to break the peptide chain. In addition, the methyl group at the N-terminal should act as a probe to ascertain the electron density at the N-terminal peptide bond in the anion. Several N-acetyl amino acids and dipeptides have been investigated by ESR. The results found for these compounds have been surprising. Reaction of the electron at 77°K produces the anion; and in every case, the unpaired electron is totally localized at the N-acetyl peptide bond. This is evidenced by the hyperfine splitting observed for the acetyl methyl group (13.5 G) which is exactly that previously observed for acetamide anion ($CH_3-\overset{\overset{O^-}{\|}}{C}-NH_2$). Warming the anions of N-acetyl amino acids or dipeptides results in the cleaving off of $CH_3-\overset{\overset{O}{\|}}{C}-\underset{\underset{H}{|}}{N^-}$ leaving a deaminated radical (as shown below for N-acetylglycyl-L-leucine).

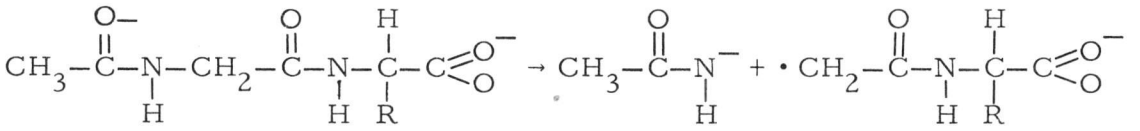

These results suggest that the cleavage of the terminal amino group in dipeptides and tripeptides is due to localization of the electron in the terminal peptide bond. For the N-acetylpeptides where a terminal amino group is not available, bond cleavage occurs at the end peptide linkage.

D. REACTIONS OF ELECTRONS WITH ESTERIFIED PEPTIDES

Localization of the extra electron at the N-terminal peptide bond in a peptide was a surprising result. It was thought that this phenomenon could arise from the fact that the carboxyl group is negatively charged before electron attachment. In this hypothesis, the electron would then migrate to the opposite end of the peptide chain and localize at the N-terminal peptide bond. To test this hypothesis, several N-acetyl peptides with their carboxyl groups esterified were reacted with the electron. Esterification of the carboxyl group removes the charge on the carboxyl group without greatly changing the structure of the peptide. It was found that electron localization again occurred at the N-terminal peptide bond. This shows that electron localization at the N-terminal peptide bond is not a result of charge repulsion. This suggests an inherent property of the electronic structure of the peptide causes localization at the N-terminal. This work is complete.

E. RADIOLYSIS OF FROZEN AQUEOUS SOLUTIONS OF CELL NUCLEI AT 77°K

Techniques have been developed for the irradiation of biological materials in frozen water suspensions at 77°K. In a preliminary experiment, cell nuclei have been investigated. Irradiation of a frozen suspension of mouse nuclei produced a large ESR signal due to the hydroxyl radical and a smaller singlet due to attack on the nuclei. Warming the sample to -130°C caused the hydroxyl radical to disappear. The singlet arising from the nuclei remained until -40°C. Some resolution was observed for spectra at -90°C. Further work should

determine the nature of the radical species associated with the resolved hyperfine structure. In a second experiment, ascites tumor cell nuclei in a formate buffer were γ-irradiated at 77°K. Results showed that the formate buffer protected the nuclear material from free radical attack. Since radicals associated with the ascites tumor nuclei were not found, we conclude that the radical species observed in irradiated mouse nuclei (without the buffer) most likely arise from the indirect effect. This work is continuing.

IV. EVALUATION OF EFFORT TO DATE

The studies of reactions of electrons with peptides in alkaline glasses has been very useful in determining the mechanism of action of this radiolytic intermediate. The result of electron attachment is found to be localization in the N-terminal peptide bond followed by deamination of the N-terminal amino group. Upon warming the alkaline glass, the deaminated radical is found to react with the parent compound to form the species usually observed in the radiolysis of solid peptides. The characterization of these radical species suggests a stepwise mechanism which explains the results of radiolysis of small peptides. In addition, it is proposed that this mechanism applies to even larger peptides. This work is complete. Techniques for the study of the radiolysis of wet chromosomes have been developed, and initial experiments have been completed on cell nuclei.

V. NEXT REPORT PERIOD ACTIVITIES

In the experimental program, chromosome constituents including DNA and peptides will be exposed to photolytically-generated electrons and hydroxyl radicals. A new photochemical method of generating and studying the reactions of both electrons and hydroxyl radicals in the liquid state will be employed. In this method, intermediates will be generated in an aqueous flow system which will permit obtaining the ESR spectra of the radicals formed. Electrons will be generated by the 2537 Å photolysis of $Fe(CN)_6^{-4}$ in neutral solution. Hydroxyl radicals will be generated by the photolysis of water at 1470 Å.[31] The photolysis cell and flow system to be used in this study have been constructed.

Chromosomes will be ^{60}Co γ-irradiated in an ice matrix at 77°K. At this temperature, anions and other radical species should be stabilized. From our work on constituents, it is known that as the temperature increases these radical species will react through deamination, protonation, and abstraction. Evidence of these reactions in chromosomes will be sought. ESR spectra, taken as a function of temperature, will be compared for chromosomes which were swollen prior to freezing (by adding a salt or by a change in pH) with those in a condensed state. In addition to providing a basis for comparison for our previour work on chromosome constituents, such a study might elucidate whether the protein component protects the DNA component in the swollen state as well as in the condensed state.